

Explicit matrices for a composite beam-column with refined zigzag kinematics

Original

Explicit matrices for a composite beam-column with refined zigzag kinematics / Wimmer, Heinz; Gherlone, Marco. - In: ACTA MECHANICA. - ISSN 0001-5970. - ELETTRONICO. - 228:6(2017), pp. 2107-2117. [10.1007/s00707-017-1816-5]

Availability:

This version is available at: 11583/2689765 since: 2019-07-09T16:17:32Z

Publisher:

Springer-Verlag Wien

Published

DOI:10.1007/s00707-017-1816-5

Terms of use:

This article is made available under terms and conditions as specified in the corresponding bibliographic description in the repository

Publisher copyright

Springer postprint/Author's Accepted Manuscript

This version of the article has been accepted for publication, after peer review (when applicable) and is subject to Springer Nature's AM terms of use, but is not the Version of Record and does not reflect post-acceptance improvements, or any corrections. The Version of Record is available online at: <http://dx.doi.org/10.1007/s00707-017-1816-5>

(Article begins on next page)

Explicit matrices for a composite beam-column with refined zigzag kinematics

Heinz Wimmer

MPT Engineering GmbH, Im Reith 34, 4221 Steyregg, Austria

Carinthia University of Applied Sciences

Villacher Str. 1, A-9800 Spittal, Austria

Tel : [+43- 6503351246](tel:+43-6503351246)

Email: heinz.wimmer@gmail.com

Marco Gherlone

Politecnico di Torino, Department of Mechanical and Aerospace Engineering

Corso Duca degli Abruzzi, 24, 10129, Torino, Italy

Tel : [+39 - 0110906817](tel:+39-0110906817)

Fax : [+39 - 0110906899](tel:+39-0110906899)

Email: marco.gherlone@polito.it

Abstract This paper presents explicit expressions of the linear and geometric stiffness matrix, as well as the mass matrix and vector of equivalent nodal forces for a simple planar beam finite element based on the Refined Zigzag Theory. After a brief review of the theory, the matrices are derived via Hamilton's principle and special anisoparametric (inter-dependent) shape functions. The C^0 -continuous element shows remarkable accuracy in the analysis of composite laminated or sandwich beams and for particular structures with partial interaction of two or more sub-components with interlayer slip.

Introduction

The high stiffness-to-weight and strength-to-weight ratio, together with the tailoring freedom, has led to a widespread adoption of composite materials, especially in the form of multi-layered structures [1]. The field of application ranges from aircraft to automotive components and from naval to civil constructions. In the civil engineering field, there exist many multi-part structural elements with shear compliant connections that can also be modelled as a multi-layered construction.

The high transverse-shear deformability of composite materials and the intrinsic through-the-thickness heterogeneity of multi-layered structures make a challenging task to accurately evaluate their mechanical behavior. Classical equivalent single layer theories (as the Classical Lamination Plate

Theory and the First-order Shear Deformation Theory) are easy to implement but, due to their excessively simplified kinematic assumptions, not always accurate (especially for thick and/or heterogeneous laminates) [2]. On the other hand, layerwise approaches (or even high-fidelity, three-dimensional finite element models based on commercial codes) provide excellent predictions but are computationally expensive [3,4].

An interesting compromise between accuracy and computational cost can be achieved using the so-called zigzag theories and the global-local theories [5-7]. Focusing on the first group we mention the pioneering works by Di Sciuva [8,9] and Cho [10] to the very last years [11], a large number of zigzag theories have been presented. A recently proposed approach is the Refined Zigzag Theory (RZT) for both beam [12] and plate structures [13]. At the cost of very few additional kinematic variables (one for the beam case and two for the plate case), RZT is able to model the normal distortion that is typical of laminated structures and to provide accurate global and local response predictions for isotropic, laminated composite, sandwich and functionally graded structures [14]. Several beam, plate and shell finite elements based on RZT have been proposed [15-20] with the aim of demonstrating the accuracy of the approach and the possibility to include RZT finite elements into commercial codes. Due to the kinematic assumptions, only C^0 -continuous shape functions are in fact required.

The implementation of finite elements into FEM commercial codes can be made easier if explicit expressions of the relevant matrices are available. Kosmatka derived the explicit formulas for the bending and transverse shear stiffness, incremental (or geometric) stiffness, mass and equivalent nodal force matrices for a two-node beam element based on the Timoshenko Beam Theory (TBT) [21]. Since the adopted shape functions are the exact solutions of the static equilibrium equations of TBT (when no distributed loads are present), the “exact” stiffness matrix is obtained in agreement with the results by Przemieniecki [22]. Similarly, Reddy has presented the flexural stiffness matrix and nodal forces vector for a beam element based on his third-order theory [23]. Tessler and Spiridigliozzi have developed a hierarchy of curved beam finite elements with anisoparametric (or interdependent) polynomial shape functions for the Timoshenko/Marguerre shallow beam model [24]. Explicit expressions for the stiffness and mass matrices are provided.

The scope of this work is to present, for the first time, explicit expressions for the linear and geometric stiffness as well as the mass matrices of a simple beam finite element based on the Refined Zigzag Theory and to demonstrate again the high performance quality of this approach. The outline of the paper is as follows. In Section 2 the kinematic assumptions of RZT for beams will be briefly reviewed in order to set the framework for the finite element formulation. Section 3 presents the derivation of the beam finite element equations of motion via the Hamilton’s principle and appropriate shape functions. Explicit expressions for the key matrices (linear and geometric stiffness, mass and equivalent nodal forces) are obtained. Section 4 provides an assessment of the modelling capabilities of the RZT beam finite element for the stability (buckling loads) and dynamic analysis (natural frequencies) of multilayered and sandwich structures.

Refined Zigzag Theory (RZT)

In this section, the basic assumptions of the RZT for planar beams in a (x, z) plane (x is the beam axial coordinate, z is the thickness coordinate) are briefly reviewed. The key idea is to enrich the displacement field of the Timoshenko Beam Theory (with 3 kinematic variables, namely the uniform axial displacement, $u(x)$, the deflection, $w(x)$, and the bending rotation, $\theta(x)$). In particular, the axial displacement presents an additional contribution, $\phi^{(k)}(z) \cdot \psi(x)$, which models the cross-sectional distortion typical of multilayered beams. $\phi^{(k)}(z)$ is the *zigzag function*, piecewise continuous along the thickness and depending on the layer sequence and the transverse shear moduli, $G_{xz}^{(k)}$. $\psi(x)$ is the *zigzag rotation* and measures the amplitude of the zigzag contribution to the axial displacement. For further details in the derivation of $\phi^{(k)}$, refer to [12]. Figure 1 shows the adopted notation for the lay-up and for the zigzag function in the case of a three-layer beam. Each layer has thickness $h^{(k)}$ (with the coordinate z ranging from z_{k-1} to z_k) and can exhibit a width $b^{(k)}$. The total thickness is $h = \sum_{k=1}^N h^{(k)}$, where N is the total number of physical layers. The zigzag function $\phi^{(k)}(z)$ can be defined in each layer in terms of its bottom and top values, $\phi_{k-1} = \phi^{(k)}(z_{k-1})$ and $\phi_k = \phi^{(k)}(z_k)$, respectively. The zigzag function vanishes on the bottom and top laminate surfaces [12], $\phi_0 = \phi^{(1)}(z_0) = \phi^{(1)}(-h/2) = 0$ and $\phi_N = \phi^{(N)}(z_N) = \phi^{(N)}(+h/2) = 0$ (see Figure 1).

The RZT defines the displacement field for the k th layer as follows

$$u^{(k)}(x, z) = u(x) + z \cdot \theta(x) + \phi^{(k)}(z) \cdot \psi(x) \quad (1a)$$

$$w^{(k)}(x, z) = w(x) \quad (1b)$$

The corresponding strains from linear elasticity theory yield

$$\varepsilon_x^{(k)}(x, z) = \frac{\partial u^{(k)}}{\partial x} = u_{,x}^{(k)} = u_{,x} + z \cdot \theta_{,x} + \phi^{(k)} \psi_{,x} = \begin{bmatrix} 1, z, \phi^{(k)} \end{bmatrix} \begin{Bmatrix} u_{,x} \\ \theta_{,x} \\ \psi_{,x} \end{Bmatrix} = \mathbf{S}_x \cdot \tilde{\boldsymbol{\varepsilon}}_x \quad (2)$$

$$\gamma_{xz}^{(k)}(x, z) = w_{,x}^{(k)} + u_{,z}^{(k)} = w_{,x} + \theta + \phi_{,z}^{(k)} \psi = \gamma + \beta^{(k)} \psi = \begin{bmatrix} 1, \beta^{(k)} \end{bmatrix} \begin{Bmatrix} \gamma \\ \psi \end{Bmatrix} = \mathbf{S}_{xz} \cdot \tilde{\boldsymbol{\varepsilon}}_{xz} \quad (3)$$

With the assumption that each layer is linearly elastic and orthotropic corresponding to the Cartesian coordinates (x, z) , the constitutive relations take the form

$$\sigma_x^{(k)} = E_x^{(k)} \varepsilon_x^{(k)} = E_x^{(k)} \mathbf{S}_x \tilde{\boldsymbol{\varepsilon}}_x \quad (4a)$$

$$\tau_{xz}^{(k)} = G_{xz}^{(k)} \gamma_{xz}^{(k)} = G_{xz}^{(k)} \gamma + G_{xz}^{(k)} \beta^{(k)} \psi = G_{xz}^{(k)} \mathbf{S}_{xz} \tilde{\boldsymbol{\varepsilon}}_{xz} \quad (4b)$$

The resultant stress vectors, $\tilde{\sigma}_x$ and $\tilde{\sigma}_{xz}$, and the generalized constitutive matrix are obtained with Eqs. (2) and (3) by integration over the cross section area A

$$\begin{aligned}\tilde{\sigma}_x &= \{N_x, M_x, M_\phi\} = \int_A \{\sigma_x^{(k)}, z\sigma_x^{(k)}, \phi^{(k)}\sigma_x^{(k)}\} dA = \int_A \mathbf{S}_x^T \sigma_x^{(k)} dA \\ &= \int_A \mathbf{S}_x^T E_x^{(k)} \mathbf{S}_x \tilde{\epsilon}_x dA = \int_A E_x^{(k)} \begin{bmatrix} 1 & z & \phi^{(k)} \\ z & z^2 & z\phi^{(k)} \\ \phi^{(k)} & z\phi^{(k)} & \phi^{(k)2} \end{bmatrix} dA \tilde{\epsilon}_x = \begin{bmatrix} A_{11} & B_{12} & B_{13} \\ B_{12} & D_{11} & D_{12} \\ B_{13} & D_{12} & D_{22} \end{bmatrix} \tilde{\epsilon}_x\end{aligned}\quad (5a)$$

$$\begin{aligned}\tilde{\sigma}_{xz} &= \{V_x, V_\phi\} = \int_A \{\tau_x^{(k)}, \beta^{(k)}\tau_x^{(k)}\} dA = \int_A \mathbf{S}_{xz}^T \tau_{xz}^{(k)} dA \\ &= \int_A \mathbf{S}_{xz}^T G_{xz}^{(k)} \mathbf{S}_{xz} \tilde{\epsilon}_{xz} dA = \int_A G_{xz}^{(k)} \begin{bmatrix} 1 & \beta^{(k)} \\ \beta^{(k)} & \beta^{(k)2} \end{bmatrix} dA \tilde{\epsilon}_{xz} = \begin{bmatrix} Q_{11} & Q_{12} \\ Q_{12} & Q_{22} \end{bmatrix} \tilde{\epsilon}_{xz}\end{aligned}\quad (5b)$$

Combining Eqs. (5) gives

$$\tilde{\sigma} = \begin{Bmatrix} \tilde{\sigma}_x \\ \tilde{\sigma}_{xz} \end{Bmatrix} = \begin{Bmatrix} N_x \\ M_x \\ M_\phi \\ V_x \\ V_\phi \end{Bmatrix} = \begin{bmatrix} A_{11} & B_{12} & B_{13} & 0 & 0 \\ B_{12} & D_{11} & D_{12} & 0 & 0 \\ B_{13} & D_{12} & D_{22} & 0 & 0 \\ 0 & 0 & 0 & Q_{11} & Q_{12} \\ 0 & 0 & 0 & Q_{12} & Q_{22} \end{bmatrix} \begin{Bmatrix} u_{,x} \\ \theta_{,x} \\ \psi_{,x} \\ \gamma \\ \psi \end{Bmatrix} = \mathbf{D} \begin{Bmatrix} \tilde{\epsilon}_x \\ \tilde{\epsilon}_{xz} \end{Bmatrix} = \mathbf{D} \tilde{\epsilon}\quad (6)$$

Finite Element Formulation

We derive the equations of motion via the principle of Hamilton

$$\delta \Pi = \int_{t_1}^{t_2} (\delta U + \delta V - \delta T - \delta W) dt = 0\quad (7)$$

where $\delta U, \delta V, \delta T$ and δW represent, respectively, the variation of the strain energy, of the potential energy associated with initial stress, of the kinetic energy and of the work of the external forces.

The variation of strain energy can expressed in terms of generalized stresses and strains

$$\delta U = \int_0^L (\delta \tilde{\epsilon}_x^T \tilde{\sigma}_x + \delta \tilde{\epsilon}_{xz}^T \tilde{\sigma}_{xz}) dx\quad (8)$$

where L is the beam finite element length.

The work done by the external loads is

$$\delta W = \int_0^L \delta \mathbf{u}^T \mathbf{q} \, dx \quad (9)$$

The displacement and distributed loads vector contain the following components

$$\mathbf{u}(x) = \begin{Bmatrix} u(x) \\ w(x) \\ \theta(x) \\ \psi(x) \end{Bmatrix}, \quad \mathbf{q}(x) = \begin{Bmatrix} p_x(x) \\ p_z(x) \\ m(x) \\ 0 \end{Bmatrix} \quad (10)$$

The variation of kinetic energy reads

$$\delta T = \int_0^L \int_A \rho^{(k)} (\delta \dot{u}^{(k)} \dot{u}^{(k)} + \delta \dot{w}^{(k)} \dot{w}^{(k)}) \, dA \, dx \quad (11)$$

Substituting Eqs. (1) yields

$$\delta T = \int_0^L \int_A \rho^{(k)} [(\delta \dot{u} + z \cdot \delta \dot{\theta} + \phi^{(k)} \delta \dot{\psi})(\dot{u} + z \cdot \dot{\theta} + \phi^{(k)} \dot{\psi}) + \delta \dot{w} \dot{w}] \, dA \, dx \quad (12)$$

For the mass moments of inertia we introduce the following general term

$$I_{nm} = \int_{-\frac{h}{2}}^{\frac{h}{2}} \rho^{(k)} b^{(k)} z^n (\phi^{(k)})^m \, dz \quad (13)$$

In detail we have

$$I_{00} = \int_{-\frac{h}{2}}^{\frac{h}{2}} \rho^{(k)} b^{(k)} \, dz = \sum_{k=1}^N \rho^{(k)} b^{(k)} h^{(k)} \quad (14a)$$

$$I_{10} = \int_{-\frac{h}{2}}^{\frac{h}{2}} \rho^{(k)} b^{(k)} z \, dz = \frac{1}{2} \sum_{k=1}^N \rho^{(k)} b^{(k)} h^{(k)} (z_k + z_{k-1}) \quad (14b)$$

$$I_{20} = \int_{-\frac{h}{2}}^{\frac{h}{2}} \rho^{(k)} b^{(k)} z^2 dz = \frac{1}{3} \sum_{k=1}^N \rho^{(k)} b^{(k)} (z_k^3 - z_{k-1}^3) \quad (14c)$$

$$I_{01} = \int_{-\frac{h}{2}}^{\frac{h}{2}} \rho^{(k)} b^{(k)} \phi^{(k)}(z) dz = \frac{1}{2} \sum_{k=1}^N \rho^{(k)} b^{(k)} h^{(k)} (\phi_k + \phi_{k-1}) \quad (14d)$$

$$I_{11} = \int_{-\frac{h}{2}}^{\frac{h}{2}} \rho^{(k)} b^{(k)} z \phi^{(k)}(z) dz = \frac{1}{6} \sum_{k=1}^N \rho^{(k)} b^{(k)} h^{(k)} [z_k(2\phi_k + \phi_{k-1}) + z_{k-1}(2\phi_{k-1} + \phi_k)] \quad (14e)$$

$$I_{02} = \int_{-\frac{h}{2}}^{\frac{h}{2}} \rho^{(k)} b^{(k)} \phi^{(k)2}(z) dz = \frac{1}{3} \sum_{k=1}^N \rho^{(k)} b^{(k)} h^{(k)} (\phi_k^2 + \phi_k \phi_{k-1} + \phi_{k-1}^2) \quad (14f)$$

After integration over the cross section, we can write the variation δT in compact form

$$\delta T = \int_0^L \begin{Bmatrix} \delta \dot{u} \\ \delta \dot{w} \\ \delta \dot{\theta} \\ \delta \dot{\psi} \end{Bmatrix}^T \cdot \begin{bmatrix} I_{00} & 0 & I_{10} & I_{01} \\ 0 & I_{00} & 0 & 0 \\ I_{10} & 0 & I_{20} & I_{11} \\ I_{01} & 0 & I_{11} & I_{02} \end{bmatrix} \cdot \begin{Bmatrix} \dot{u} \\ \dot{w} \\ \dot{\theta} \\ \dot{\psi} \end{Bmatrix} dx = \int_0^L \delta \dot{\mathbf{u}}^T \mathbf{R} \dot{\mathbf{u}} dx \quad (15)$$

The variation of the potential energy of the beam-column associated with a constant initial axial force F ($F > 0$ for tension) is given as

$$\delta V = F \cdot \int_0^L \delta w_{,x} w_{,x} dx \quad (16)$$

The kinematic variables $u(x)$, $w(x)$ and $\psi(x)$ are discretized using standard linear shape functions. For the deflection $w(x)$, an anisoparametric (interdependent) interpolation is chosen which guarantees that no parasitic shear strains arise in the thin limit case [15]. The approximation of the kinematic variables can be written as follows

$$\mathbf{u}(x) = \mathbf{N}(x) \cdot \mathbf{u}_e \quad (17)$$

where \mathbf{u}_e is the nodal degrees-of-freedom vector, $(u_1, w_1, \theta_1, \psi_1, u_2, w_2, \theta_2, \psi_2)$, and

$$\mathbf{N} = \begin{bmatrix} N_1^L & 0 & 0 & 0 & N_2^L & 0 & 0 & 0 \\ 0 & N_1^L & -\frac{L}{8} N_m^Q & -\frac{cL}{8} N_m^Q & 0 & N_2^L & \frac{L}{8} N_m^Q & \frac{cL}{8} N_m^Q \\ 0 & 0 & N_1^L & 0 & 0 & 0 & N_2^L & 0 \\ 0 & 0 & 0 & N_1^L & 0 & 0 & 0 & N_2^L \end{bmatrix} \quad (18)$$

With the dimensionless coordinate $\xi = \left(\frac{2x}{L} - 1\right)$ along the beam axis, the shape functions read

$$N_1^L(\xi) = \frac{1}{2}(1 - \xi), \quad N_2^L(\xi) = \frac{1}{2}(1 + \xi), \quad N_m^Q(\xi) = (1 - \xi^2) \quad (19)$$

The factor c depends on the constraint condition used to simplify the element topology to the classical one with degrees-of-freedom only defined at the beam ends. Numerical studies indicate that the best results are obtained when using the condition $V_x = \text{const.}$ [15]. In this case

$$c = Q_{12}/Q_{11} \quad (20)$$

From Eqs. (2), (3) and (18) we get the element strain matrix

$$\tilde{\boldsymbol{\epsilon}} = \begin{bmatrix} u_{,x} \\ \theta_{,x} \\ \psi_{,x} \\ \gamma \\ \psi \end{bmatrix} = \mathbf{B} \cdot \mathbf{u}_e = \begin{bmatrix} -\frac{1}{L} & 0 & 0 & 0 & \frac{1}{L} & 0 & 0 & 0 \\ 0 & 0 & -\frac{1}{L} & 0 & 0 & 0 & \frac{1}{L} & 0 \\ 0 & 0 & 0 & -\frac{1}{L} & 0 & 0 & 0 & \frac{1}{L} \\ 0 & -\frac{1}{L} & \frac{1}{2} & c\frac{\xi}{2} & 0 & \frac{1}{L} & \frac{1}{2} & -c\frac{\xi}{2} \\ 0 & 0 & 0 & \frac{1}{2}(1 - \xi) & 0 & 0 & 0 & \frac{1}{2}(1 + \xi) \end{bmatrix} \cdot \mathbf{u}_e \quad (21)$$

After substitution of Eq. (21) into Eq. (8), using (6) and subsequent integration over the beam length, the linear stiffness matrix is obtained

$$\mathbf{K}_e = \frac{L}{2} \int_{-1}^{+1} \mathbf{B}^T(\xi) \mathbf{D} \mathbf{B}(\xi) d\xi =$$

$$\begin{bmatrix} \frac{A_{11}}{L} & 0 & \frac{B_{12}}{L} & \frac{B_{13}}{L} & -\frac{A_{11}}{L} & 0 & -\frac{B_{12}}{L} & -\frac{B_{13}}{L} \\ \frac{Q_{11}}{L} & -\frac{Q_{11}}{2} & -\frac{Q_{12}}{2} & -\frac{Q_{12}}{2} & 0 & -\frac{Q_{11}}{L} & -\frac{Q_{11}}{2} & -\frac{Q_{12}}{2} \\ \frac{Q_{11}L^2+4D_{11}}{4L} & \frac{Q_{12}L^2+4D_{12}}{4L} & \frac{Q_{12}L^2-4D_{11}}{4L} & \frac{Q_{12}L^2-4D_{12}}{4L} & -\frac{B_{12}}{L} & \frac{Q_{11}}{2} & \frac{Q_{11}L^2-4D_{11}}{4L} & \frac{Q_{12}L^2-4D_{12}}{4L} \\ \left(\frac{(4Q_{22}-2cQ_{12}+c^2Q_{11})L}{12} + \frac{D_{22}}{L}\right) & -\frac{B_{13}}{L} & \frac{Q_{12}}{2} & \frac{Q_{12}L^2-4D_{12}}{4L} & \frac{A_{11}}{L} & 0 & \frac{B_{12}}{L} & \frac{B_{13}}{L} \\ \frac{A_{11}}{L} & 0 & \frac{Q_{11}}{L} & \frac{Q_{11}}{2} & -\frac{B_{12}}{L} & \frac{Q_{11}}{2} & \frac{Q_{11}L^2+4D_{11}}{4L} & \frac{Q_{12}L^2+4D_{12}}{4L} \\ \frac{Q_{11}L^2+4D_{11}}{4L} & \frac{Q_{12}L^2+4D_{12}}{4L} & \frac{Q_{12}L^2-4D_{11}}{4L} & \frac{Q_{12}L^2-4D_{12}}{4L} & -\frac{B_{12}}{L} & \frac{Q_{11}}{2} & \frac{Q_{11}L^2-4D_{11}}{4L} & \frac{Q_{12}L^2-4D_{12}}{4L} \\ \left(\frac{(4Q_{22}-2cQ_{12}+c^2Q_{11})L}{12} + \frac{D_{22}}{L}\right) & -\frac{B_{13}}{L} & \frac{Q_{12}}{2} & \frac{Q_{12}L^2-4D_{12}}{4L} & \frac{A_{11}}{L} & 0 & \frac{B_{12}}{L} & \frac{B_{13}}{L} \end{bmatrix}$$

Symm.

$$(22)$$

For the derivation of the consistent load vector, linearly varying loads are assumed

$$\mathbf{q}(x) = \begin{Bmatrix} p_{x1}N_1^L(\xi) + p_{x2}N_2^L(\xi) \\ p_{z1}N_1^L(\xi) + p_{z2}N_2^L(\xi) \\ m_1N_1^L(\xi) + m_2N_2^L(\xi) \\ 0 \end{Bmatrix} \quad (23)$$

From Eq. (9) it follows

$$\mathbf{f}_e = \frac{L}{2} \int_{-1}^{+1} \mathbf{N}(\xi)^T \mathbf{q}(\xi) d\xi = \begin{Bmatrix} \frac{L}{6}(2p_{x1} + p_{x2}) \\ \frac{L}{6}(2p_{z1} + p_{z2}) \\ -\frac{(p_{z1}+p_{z2})L^2-(8m_1+4m_2)L}{24} \\ -\frac{c(p_{z1}+p_{z2})L^2}{24} \\ \frac{L}{6}(p_{x1} + 2p_{x2}) \\ \frac{L}{6}(p_{z1} + 2p_{z2}) \\ \frac{(p_{z1}+p_{z2})L^2+(4m_1+8m_2)L}{24} \\ \frac{c(p_{z1}+p_{z2})L^2}{24} \end{Bmatrix} \quad (24)$$

Substituting the interpolations

$$\dot{\mathbf{u}} = \mathbf{N} \dot{\mathbf{u}}_e \quad (25)$$

$$\delta \dot{\mathbf{u}} = \mathbf{N} \delta \dot{\mathbf{u}}_e \quad (26)$$

we finally get the expression for the variation of the kinetic energy

$$\delta T = \delta \dot{\mathbf{u}}_e^T \int_0^L \mathbf{N}^T \mathbf{R} \mathbf{N} dx \dot{\mathbf{u}}_e = \delta \dot{\mathbf{u}}_e^T \mathbf{M} \dot{\mathbf{u}}_e \quad (27)$$

and of the mass matrix

$$\begin{aligned}
\mathbf{M} &= \frac{L}{2} \int_{-1}^{+1} \mathbf{N}^T(\xi) \mathbf{R} \mathbf{N}(\xi) d\xi = \\
&\frac{L}{120} \cdot \begin{bmatrix}
40I_{00} & 0 & 40I_{10} & 40I_{01} & 20I_{00} & 0 & 20I_{10} & 20I_{01} \\
& 40I_{00} & -5I_{00}L & -5cI_{00}L & 0 & 20I_{00} & 5I_{00}L & 5cI_{00}L \\
& & I_{00}L^2 + 40I_{20} & cI_{00}L^2 + 40I_{11} & 20I_{10} & -5I_{00}L & 20I_{20} - I_{00}L^2 & 20I_{11} - cI_{00}L^2 \\
& & & c^2I_{00}L^2 + 40I_{02} & 20I_{01} & -5cI_{00}L & 20I_{11} - cI_{00}L^2 & 20I_{02} - c^2I_{00}L^2 \\
& & & & 40I_{00} & 0 & 40I_{10} & 40I_{01} \\
& & & & & 40I_{00} & 5I_{00}L & 5cI_{00}L \\
& & & & & & I_{00}L^2 + 40I_{20} & cI_{00}L^2 + 40I_{11} \\
& & & & & & & c^2I_{00}L^2 + 40I_{02}
\end{bmatrix} \\
&\text{Symm.}
\end{aligned}
\tag{28}$$

The initial stiffness matrix \mathbf{K}_G is developed by using the interdependent shape function \mathbf{N}_w for the transversal deflection $w(x)$ as given in the second row of Eq. (18)

$$\mathbf{N}_w = \left[0, N_{1L}, \left(-\frac{L}{8} N_m^Q\right), \left(-\frac{cL}{8} N_m^Q\right), 0, N_{2L}, \left(-\frac{L}{8} N_m^Q\right), \left(-\frac{cL}{8} N_m^Q\right) \right]
\tag{29}$$

$$\begin{aligned}
\delta V &= F \cdot \int_0^L \delta w_{,x} w_{,x} dx = F \cdot \int_0^L (\mathbf{N}_{w,x} \delta \mathbf{u}_e)^T (\mathbf{N}_{w,x} \mathbf{u}_e) dx = \delta \mathbf{u}_e^T \left[F \cdot \int_0^L \mathbf{N}_{w,x}^T \mathbf{N}_{w,x} dx \right] \mathbf{u}_e \\
&= \delta \mathbf{u}_e^T \mathbf{K}_G \delta \mathbf{u}_e
\end{aligned}
\tag{30}$$

$$\mathbf{K}_G = \int_0^L \mathbf{N}_{w,x}^T \mathbf{N}_{w,x} dx = \frac{L}{2} \int_{-1}^{+1} \mathbf{N}_{w,x}^T(\xi) \mathbf{N}_{w,x}(\xi) d\xi
\tag{31}$$

After integration we obtain the explicit form of the initial stiffness matrix

$$\mathbf{K}_G = \frac{F}{12L} \cdot \begin{bmatrix}
0 & 0 & 0 & 0 & 0 & 0 & 0 & 0 \\
& 12 & 0 & 0 & 0 & -12 & 0 & 0 \\
& & L^2 & cL^2 & 0 & 0 & L^2 & -cL^2 \\
& & & c^2L^2 & 0 & 0 & -cL^2 & -c^2L^2 \\
& & & & 0 & 0 & 0 & 0 \\
& & & & & 12 & 0 & 0 \\
& & & & & & L^2 & cL^2 \\
& & & & & & & c^2L^2
\end{bmatrix}
\tag{32}$$

Symm.

The finite element equation of motion then reads

$$\mathbf{M} \ddot{\mathbf{u}}_e + (\mathbf{K} + \mathbf{K}_G) \mathbf{u}_e = \mathbf{f}_e
\tag{33}$$

As a special case we get from Eq. (33) the equation for the linear stability analysis

$$(K - \lambda K_G)u_e = 0 \quad (34)$$

and the equation representing the free vibration analysis

$$(K - \omega^2 M)u_e = 0 \quad (35)$$

Numerical Results

As a first example, we demonstrate the applicability of RZT beam finite elements to a structure which is normally analyzed by the theory of beam-columns with partial interaction of two subcomponents. Among others, Girhammer et al. [25-27] have given analytical expressions for such a composite beam-column with interlayer slip where Bernoulli's hypothesis is used for each component. Adam et al. [28] have dealt with the same beam under sinusoidal and random excitations. Xu et al. [29] have developed a model with reference to Timoshenko's theory, Kryzanowski et al. [30] proposed a mathematical model for slip buckling and Grenoc et al. [31] gave recently a two-layer beam solution for the buckling load based on Timoshenko's theory. We refer to the work of Langosch [32] who compared different slip theories when dealing with laminated glass constructions.

The interlayer slip s , as a relative displacement between the two subcomponents, will be driven by the shear load per unit length q via the following linear relation

$$q(x) = K_s \cdot s(x) \quad (36)$$

where K_s stands for the stiffness of the shear connectors (slip modulus). If we model the slipping zone by a weak interlayer with thickness t , the interlayer slip s can be evaluated with the following linearized relation

$$s(x) \cong \gamma(x) \cdot t = \frac{\tau(x)}{G_f} \cdot t = \frac{q(x)}{b \cdot G_f} \cdot t \quad (37)$$

In Eq. (37), γ and τ denote the mean value of the shear angle and of the shear stress of the weak interlayer, G_f denotes the shear modulus, b is the width of the same layer. Substituting Eq. (37) into Eq. (36), we get the following relation [32]

$$K_s = \frac{G_f b}{t} \quad (38)$$

We investigate the buckling of two different beam-columns composed of two and three glass panes, respectively, and with one or two sheets of Polyvinylbutyral (PVB), which is approximately assumed as elastic (see Figure 2). Further geometrical and mechanical properties of the columns are: beam length $L = 2000$ mm; glass: $E_{x,g} = 70000$ N/mm²; $G_{xz,g} = 28460$ N/mm²; PVB: Poisson's ratio $\nu_f = 0.39$. Two different shear moduli G_f are used for the isotropic interlayer (see Tables 1, 2).

Table 1 shows the convergence of buckling load values obtained by the proposed FE-model compared with a slip model and with a high precision 2D-FE analysis when using a pinned-pinned support condition. For the special case of constrained warping at the supports, no analytical solution does exist. The RZT-model allows easily to distinguish two variants of warping behaviour of the end cross section by controlling the fourth kinematic degree, $\psi(x)$, which activates or deactivates the internal zigzag kinematic (Figure 3 and Figure 4). In Table 2 the buckling load values $F_{b,con}$ are given for the case when the slip at the end of the beam is constrained (F_b denotes the buckling load without end constraint). Parametric studies [32] have shown that the increasing effect Δ to the buckling resistance when constraining the warping of beam's end cross section depends on

- the shear modulus of interlayer;
- the buckling length;
- the thickness of panes.

The second example deals with the free vibration of a cantilever sandwich beam for which experimental data exist. For the detailed description of the experimental setup and tests, refer to [33]. The beam has an effective span of $L = 32$ cm and the symmetric cross section (width $b = 48.53$ mm) consists of three layers with a core thickness of 6.07 mm and two faces with 5.00 mm. Core and faces exhibit the following material data (Table 3).

In Table 4 the first five experimental natural frequencies are reported and compared with the results provided by the present RZT FE solution (for an increasing number of elements). The presence of the ten accelerometers is also taken into account by considering lumped masses (1.45 g) located at the right positions along the beam span ($x = 3, 47, 80, 113, 145, 180, 212, 245, 278$ and 315 mm). For sake of comparison, Table 4 also shows the first five natural frequencies evaluated by a high-fidelity plane-stress FE solution based on 20480 QUAD8 parabolic elements (10 elements through the thickness of each face, 12 elements through the thickness of the core and 640 elements along the span). The commercial package MSC/PATRAN and NASTRAN has been used.

The comparison between the NASTRAN and RZT natural frequencies reveals that the latter are accurate even if using few beam elements (10). In order to obtain similar performances on the higher-order modes, more elements are required (50) but the computational effort is again much less

demanding with respect to the NASTRAN model. The difference between numerical (RZT and NASTRAN) and experimental frequencies is somehow higher (5% on the fundamental frequency, 7% on the second one and less than 5% the other ones) but this can be due to the mechanical properties of the core material that have been evaluated through an experimental procedure [33] that revealed a not negligible statistical dispersion.

Since the present RZT-based beam finite element corresponds to the one proposed in [15] (with the constraint $V_x = \text{const.}$), the same numerical examples discussed in this section have been analyzed with the original element and found to provide results coinciding with the current ones.

Conclusions

In the present paper, the explicit expressions of the linear and geometric stiffness matrix, as well as the mass matrix and vector of equivalent nodal forces, are derived for a simple beam finite element based on the Refined Zigzag Theory for the analysis of composite laminated and sandwich structures.

The theory is briefly reviewed and the finite element formulation is presented. A set of numerical results is also discussed in order to assess the accuracy of the approach with respect to high-fidelity 2D FE models built using commercial codes and to experimental tests. Buckling loads of compressed composite beam-columns and natural frequencies of sandwich beams are evaluated.

For both applications, RZT-based finite elements show to be accurate with a reduced computational cost (if compared to detailed 2D FE models) and slightly more demanding with respect to beam finite elements usually implemented in commercial codes (based on the Timoshenko Beam Theory). Moreover, the availability of explicit expressions for the key FE matrices makes the proposed finite element a useful approach for the analysis of static, dynamic and stability analysis of multilayered composite beams.

References

- [1] Altenbach, H. et al.: Mechanics of Composite Structural Elements. Springer, Berlin 2004
- [2] Reddy, J.N.: Mechanics of Laminated Composite Plates and Shells. 2nd Edition, CRC Press 2004
- [3] Reddy, J.N.: A Generalization of Two-Dimensional Theories of Laminated Composite Plates. Comm. Appl. Num. Meth. **3**(3), 173-180 (1987)
- [4] Lu, X., and Liu, D.: An Interlaminar Shear Stress Continuity Theory for both Thin and Thick Composite Laminates. J. Appl. Mech. **59**(3), pp. 502-509 (1992)

- [5] Li X., Liu D.: Generalized laminate theories based on double superposition hypothesis. *Int. J. Num. Meth. Eng.* **40**, 1197-1212 (1997)
- [6] Shariyat M.: A generalized global-local high-order theory for sandwich plates subjected to thermo-mechanical loads. *Int. J. Mech. Sci.* **52**, 495-514 (2010)
- [7] Lezgy-Nazagah, M., Shariyat, M., Beheshti-Aval, S.B.: A refined high-order global-local theory for the finite element bending and vibration analysis of laminated composite beams. *Acta Mechanica* **217**, 219-242 (2011)
- [8] Di Sciuva, M.: Development of an anisotropic, multilayered, shear-deformable rectangular plate element. *Computers & Structures* **21**(4), 789-796 (1985)
- [9] Di Sciuva, M.: Multilayered anisotropic plate models with continuous interlaminar stresses. *Composite Structures* **22**(3), 149-167 (1992)
- [10] Cho, M., Parmenter, R.R.: Efficient Higher Order Composite Plate Theory for General Lamination Configurations. *AIAA J.* **31**(7), 1299-1306 (1993)
- [11] Icardi, U., Sola, F.: Assessment of recent zig-zag theories for laminated and sandwich structures. *Composites Part B: Engineering* **97**, 26-52 (2016)
- [12] Tessler A., Di Sciuva, M., Gherlone, M.: A refined zigzag beam theory for composite and sandwich beams, *Journal of Composite Materials* **43**(9), 1051-1081 (2009)
- [13] Tessler, A., Di Sciuva, M., Gherlone, M.: A consistent refinement of first-order shear-deformation theory for laminated composite and sandwich plates using improved zigzag kinematics. *Journal of Mechanics of Materials and Structures* **5**(2), 341-367 (2010)
- [14] Iurlaro L., Gherlone, M., Di Sciuva, M.: Bending and free vibration analysis of functionally graded sandwich plates using the Refined Zigzag Theory. *Journal of Sandwich Structures and Materials* **16**(6), 669-699 (2014)
- [15] Gherlone, M., Tessler, A., Di Sciuva, M.: C0 beam elements based on Refined Zigzag Theory for multilayered composite and sandwich laminates. *Composite Structures* **93**, 2882-2894 (2011)
- [16] Onate E., Eijo A., Oller S.: Simple and accurate two-noded beam element for composite laminated beams using a refined zigzag theory. *Comp. Methods Appl. Mech. Engrg.* **213-216**, 362-382 (2012)
- [17] Di Sciuva M., Gherlone M., Iurlaro L., Tessler A.: A class of higher-order C0 composite and sandwich beam elements based on the Refined Zigzag Theory. *Composite Structures* **132**, 784-803 (2015)
- [18] Versino, D., Mattone, M., Gherlone, M., Tessler, A., and Di Sciuva, M.: An efficient C0 triangular elements based on the Refined Zigzag Theory for multilayered composite and sandwich plates. *Composites Part B* **44**(1), 218-230 (2013)

- [19] Versino D., Gherlone M., Di Sciuva M.: Four-node shell element for doubly curved multilayered composites based on the Refined Zigzag Theory, *Composite Structures* **118**, 392-402 (2014)
- [20] Flores, F.G.: Implementation of the refined zigzag theory in shell elements with large displacements and rotations. *Composite Structures* **118**, 560-570 (2014)
- [21] Kosmatka, J.B.: An improved two-node finite element for stability and natural frequencies of axial-loaded Timoshenko-beams. *Computer & Structures* **57**(1), 141-149 (1995)
- [22] Przemieniecki J.S.: *Theory of Matrix Structural Analysis*. McGraw-Hill, New York (1968)
- [23] Reddy, J.N.: On locking-free shear deformable beam finite elements. *Comp. Methods Appl. Mech. Engrg* **149**, 113-132 (1997)
- [24] Tessler, A., Spiridigliozzi L.: Curved Beams with penalty relaxation. *International Journal for Numerical Methods in Engineering* **23**, 2245-2262 (1986)
- [25] Girhammer, U.A., Gopu V.K.A.: Composite Beam-Columns with Interlayer Slip – Exact Analysis. *Journal of Structural Engineering* **119**(4), 1265-1282 (1993)
- [26] Girhammer, U.A., Pan D.: Dynamic Analysis of Composite Members with Interlayer Slip. *International Journal of Solids and Structures* **30**(6), 797-823 (1993)
- [27] Girhammer, U.A., Pan D.: Exact static analysis of partially composite beams and beam-columns. *International Journal of Mechanical Sciences* **49**, 239-255 (2007)
- [28] Adam C., Heuer R., Jeschko A: Flexural vibrations of elastic composite beams with interlayer slip. *Acta Mechanica* **125**, 17-30 (1997)
- [29] Xu R., Wu Y.: Static, dynamic and buckling analysis of partial interaction composite members using Timoshenko's beam theory. *International Journal of Mechanical Sciences* **49**, 1139-1155 (2007)
- [30] Kryzanowski A., Schnabl S., Turk G., Planinc I.: Exact slip-buckling analysis of two-layer composite columns. *International Journal of Solids and Structures* **46**, 2929-2938 (2009)
- [31] Le Grenoc, P., Nguyen Q., Hjiat M.: Exact buckling solution for two-layer Timoshenko beams with interlayer slip. *International Journal of Solids and Structures* **49**, 143-150 (2012)
- [32] Langosch, K.P.: *Das Tragverhalten von Glasstützen mit Mono- und Verbundquer-schnitten*. PhD Thesis (in german). RWTH Aachen (2013)
- [33] Iurlaro L., Ascione A., Gherlone, M., Mattone M., Di Sciuva, M.: Free vibration analysis of sandwich beams using the Refined Zigzag Theory: an experimental assessment. *Meccanica* **50**, 2525-2535 (2015)

Figure captions

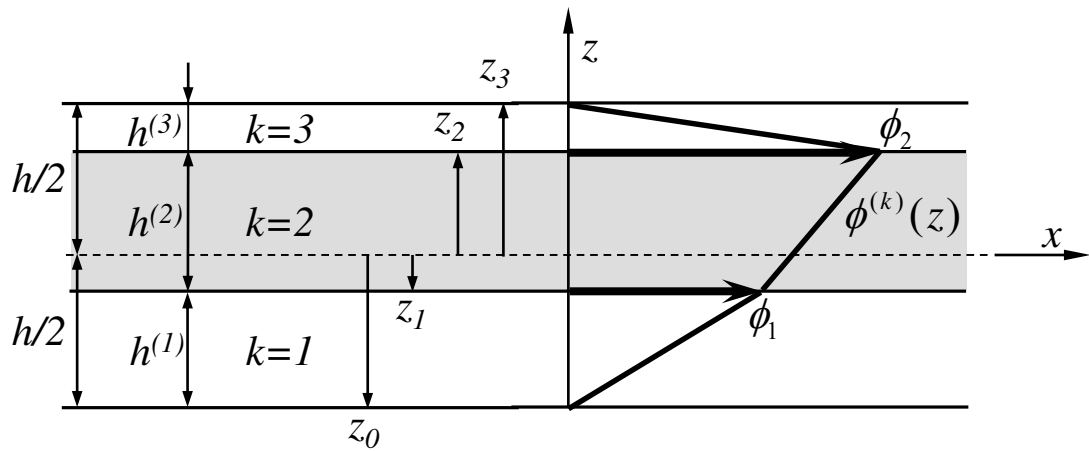
Fig.1 Lay-up notation and zigzag function for a three-layer beam.

Fig.2 Cross sections of laminated glass beam-columns.

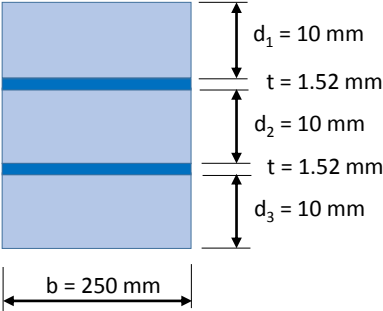
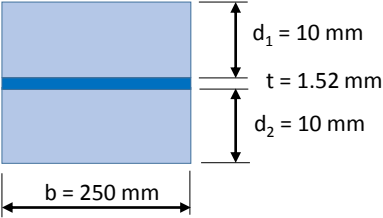
Fig.3 Pinned support with and without warping and slip, respectively.

Fig.4 Buckling modes of a pinned-pinned beam-column (three-layer laminated safety glass) with/without slip constraint at the beam's end.

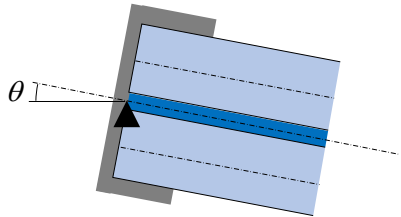
Figure



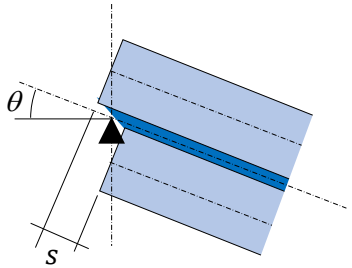
Figure



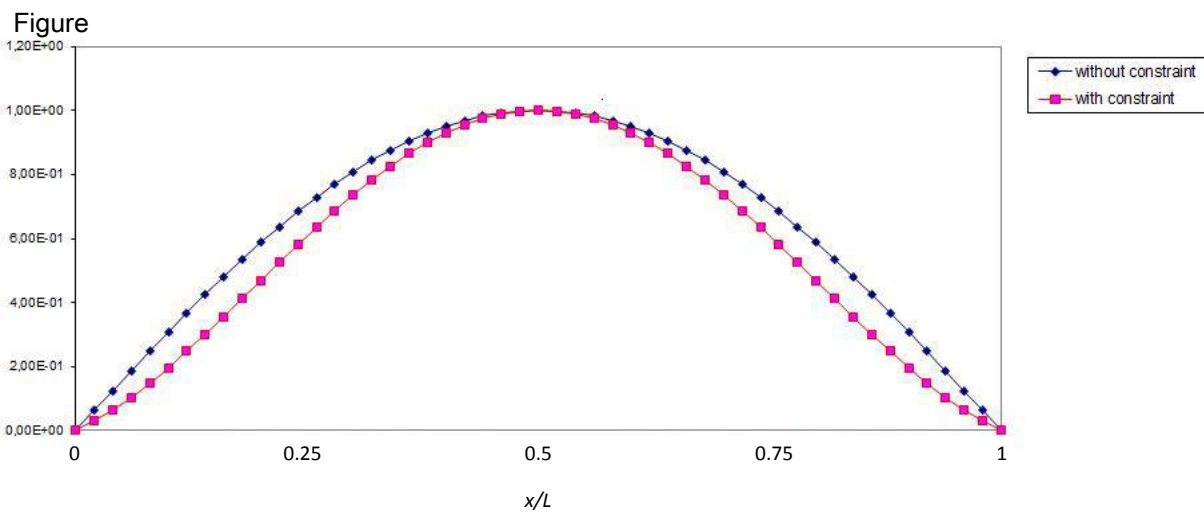
Figure



$\psi = 0, s = 0$



$\psi \neq 0, s \neq 0$



Shear modulus of PVB interlayer		Linear buckling load F_b for two-layer laminated safety glass ($d_1 = d_2$)						
		5 El.	10 El.	20 El.	50 El.	100 El.	Slip theory [32]	FE (2D) [32]
$G_f = 1$ N/mm ²	[kN]	20.00	19.69	19.61	19.59	19.58	19.59	19.55
$G_f = 10$ N/mm ²	[kN]	33.5	32.76	32.58	32.53	32.52	32.52	32.24
		Linear buckling load F_b for three-layer laminated safety glass ($d_1 = d_2 = d_3$)						
		5 El.	10 El.	20 El.	50 El.	100 El.	Slip theory [32]	FE (2D) [32]
$G_f = 1$ N/mm ²	[kN]	43.04	42.56	42.44	42.41	42.40	42.41	42.40
$G_f = 10$ N/mm ²	[kN]	104.27	102.22	101.70	101.56	101.54	101.57	101.58

Table 1 Buckling loads F_b without slip constraint at the end of beam ($\psi \neq 0$).

Shear modulus of PVB interlayer		Linear buckling load $F_{b,con}$ for two-layer laminated safety glass ($d_1 = d_2$)					$\Delta = \frac{F_{b,con} - F_b}{F_b}$
		5 El.	10 El.	20 El.	50 El.	100 El.	(%)
$G_f = 1$ N/mm ²	[kN]	26.55	25.43	25.17	25.10	25.09	+28.1
$G_f = 10$ N/mm ²	[kN]	34.51	33.46	33.20	33.13	33.12	+1.8
		Linear buckling load $F_{b,con}$ for three-layer laminated safety glass ($d_1 = d_2 = d_3$)					$\Delta = \frac{F_{b,con} - F_b}{F_b}$
		5 El.	10 El.	20 El.	50 El.	100 El.	(%)
$G_f = 1$ N/mm ²	[kN]	62.91	60.01	59.34	59.15	59.13	+39.5
$G_f = 10$ N/mm ²	[kN]	110.21	106.31	105.33	105.05	105.01	+3.4

Table 2 Buckling loads $F_{b,con}$ with slip constraint at the end of beam ($\psi = 0$).

Material	E (N/mm ²)	G (N/mm ²)	ρ (kg/m ³)
Ergal® (faces)	69570	25766	2849
Rohacell® IG31 (core)	40.3	12.4	36.825

Table 3 Mechanical material properties (mean values, refer to [33]): Young’s modulus, shear modulus and mass density.

Mode	Experimental (Hz)	Refined Zigzag Theory			NASTRAN
		10 Elem.	50 Elem.	100 Elem.	20480 Elem.
1	88.3	84.3	84.0	83.9	83.9
2	357	336	332	331	331
3	804	803	773	771	771
4	1414	1523	1412	1408	1407
5	2214	2582	2263	2252	2250

Table 4 First natural frequencies of specimen IG31_32_5. Experimental frequencies are different from those shown in [33] (Table 3) since the latter were not correctly reported.